Economic Operation of Integrated Energy Systems Considering Combined Production of Hydrogen and Medical Oxygen

Ding, Haohui; Hu, Qinran; Ge, Yi; Wu, Qiuwei; Dou, Xiaobo; Li, Yang

Published in:
IET Renewable Power Generation

Link to article, DOI:
10.1049/iet-rpg.2020.0331

Publication date:
2021

Document Version
Peer reviewed version

IET Research Journals

Submission Template for IET Research Journal Papers

IET Journals
The Institution of Engineering and Technology

Economic Operation of Integrated Energy Systems Considering Combined Production of Hydrogen and Medical Oxygen

ISSN 1751-8644
doi: 0000000000
www.ietdl.org

Haohui Ding[1], *Qinran Hu*[*1,2], *Yi Ge*[3], *Qiuwei Wu*[4], *Xiaobo Dou*[1], *Yang Li*[1]

[1] *School of Electrical Engineering, Southeast University, China*
[2] *Jiangsu Provincial Key Laboratory of Smart Grid Technology and Equipment, China*
[3] *State Grid Jiangsu Economic Research Institute, China*
[4] *Department of Electrical Engineering, Technical University of Denmark, Denmark*
* *E-mail: qhu@seu.edu.cn*

Abstract: Developing integrated energy systems has been considered a feasible pathway to renewable-powered energy systems. The power to hydrogen technology is recognized as a promising method to enhance the economics of integrated energy systems and help reduce renewable curtailments. However, oxygen-enriched gas, which is the by-product of power to hydrogen processes (electrolysation), has not been fully utilized yet. It can be purified to produce medical oxygen at a low cost and may further increase the economics of integrated energy systems. Particularly, at this very moment, the consideration of the combined production of hydrogen and medical oxygen also has the potential in relieving the shortage of medical oxygen due to the outbreak of the 2019 novel coronavirus (COVID-19). This paper proposes a model for the operation of integrated energy systems which considers the combined production of hydrogen and medical oxygen. This model is formulated as a convex mixed-integer optimization problem which balances the electricity, heat and hydrogen demands every hour in a 24-hour period and balances oxygen demand on a daily basis. In order to find the global optimal solution, this paper uses *Yalmip* calling *Gurobi* to seek the most economic unit dispatch strategy. A test case of Taizhou City has been studied and showed that the combined production of hydrogen and medical oxygen improves the integrated energy system economics.

1 Introduction

The transition to renewable-powered energy systems has become a global trend [1]. The uncertainty of renewables raises natural concerns of maintaining the real-time balance between energy demand and supply, along with reducing the curtailment of renewables. As integrated energy systems(IES) include various devices and couples heating and electricity systems, they can help improve the operating flexibility of energy systems [2, 3]. Thus, developing IES has been considered a feasible pathway to reliable and economic renewable-powered energy systems [4].

In recent years, the power to hydrogen (P2H) is recognised as a promising method to enhance the economics of IES further, and help reduces renewable curtailments [3]. Because hydrogen can generate heat and electricity, produce methane, and power fuel cell vehicles [5]. Currently, excess renewable energy is recognized as a suitable energy source for P2H [6], and researchers usually use mixed-integer models to evaluate the economics of this measure [3]. In practice, P2H in IES is realized by electrolysing water. The electrolysation of water produces hydrogen along with a significant amount of oxygen-enriched gas, which has not been fully utilized. Processed by oxygen-enriched gas purification device, oxygen-enriched gas can be converted to medical oxygen at a low cost. The conventional method of producing medical oxygen, the cryogenic separation method, consumes 0.61 kWh electricity for 1 kg medical oxygen [7], while purification of oxygen-enriched gas consumes 0.04 kWh electricity for 1 kg medical oxygen. Therefore, in the long run, the consideration of the combined production of hydrogen and medical oxygen may further increase the economics of IES.

Besides, COVID-19 has infected more than 8 million people worldwide [8], and breathing medical oxygen has been considered as an effective treatment to help reduce the mortality rate of COVID-19 patients [9]. Numerous patients breathe medical oxygen through ventilators or extracorporeal membrane oxygenation (ECMO), which causes a dramatic increase in medical oxygen demand. Naturally, in the areas with severe epidemics, the supply of medical oxygen is insufficient [10]. Thus, at this very moment, the consideration of the combined production of hydrogen and medical oxygen also has the potential in relieving the shortage of medical oxygen.

To study the impact of combined production of hydrogen and medical oxygen, this paper proposes an optimal operation model of heat, electricity, hydrogen and oxygen for an IES which includes electric boiler, electrolyser, hydrogen storage tank, oxygen-enriched gas purification device and energy storage device. The proposed model simulates the interaction of power system with heat system, optimizes the electrical, thermal, hydrogen, oxygen outputs of all units under the market operation. In this model, the balance of electrical, thermal, hydrogen demands are on an hourly basis, and the balance of oxygen is on a daily basis because oxygen stores in oxygen cylinders which does not require real-time balance.

This is the first paper to consider the utilization of the by-product of P2H, oxygen-enriched gas, which is untapped asset in the P2H process in the past. The contributions of this paper can be summarized as follows:

1)This paper explores a new power-to-hydrogen-and-oxygen(P2HO) system that can fully utilise oxygen-enriched gas, the by-product of P2H system. The P2HO system can produce medical oxygen at a lower cost compared to the traditional cryogenic separation method.

2) Considering the proposed P2HO system can improve IES economics, this paper provides a solution of the P2HO system integration into the existing IES system, and formulates an integrated power, heat, hydrogen and oxygen

optimization (IPHHOO) model, which emulates the P2HO-involved IES operation.

3) Based on the IPHHOO model, this paper studies the impact of combined production of hydrogen and medical oxygen on the economics of IES and sensitivity analysis is given subsequently.

The remainder of this paper is organized as follows. The models of P2HO system are described in Section 2. The optimization model of integrated power, heat, hydrogen, and oxygen are detailed in Section 3. In Section 4, the impact of combined production of hydrogen and medical oxygen is analyzed with simulation results based on Taizhou. Section 5 concludes the paper.

2 P2HO system

The P2HO system is based on typical P2H system and realises the combined production of hydrogen and medical oxygen. The P2HO system contained an alkaline electrolyser, an hydrogen storage tank, and an oxygen-enriched gas purification device. The models of these devices are shown as follows.

2.1 Alkaline electrolyser

The alkaline electrolyser is the most mature and feasible method for electrolysing water. A typical P2HO system containing an alkaline electrolyser is shown in Fig. 1.

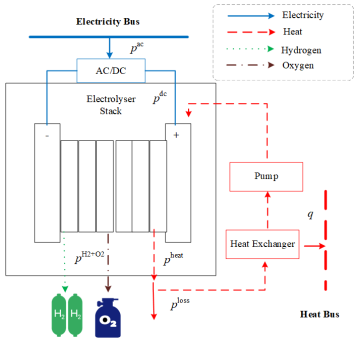

Fig. 1: Schematic of alkaline electrolyser

The entire system in Fig. 1 includes three energy sources. The electrical network supplies power $p_{i,t}$ to the electrolyser and is converted to $\mathrm{p}_{i,t}^{dc}$ by an AC/DC converter, with a conversion efficiency of $\eta_{i,1}$. Through the electrochemical reaction of an alkaline electrolyser, a portion of the electrical energy $p_{i,t}^{H_2}$ is used to produce hydrogen and another portion is converted to thermal energy $p_{i,t}^{heat}$, as shown in eq.(1):

$$\mathrm{p}_{i,t}^{dc} = p_{i,t}^{H_2} + p_{i,t}^{heat} \tag{1}$$

The model of the electrolysis process consists of two submodels, the electrochemical and thermal submodels.

2.1.1 Electrochemical submodel: The electrochemical reaction is shown in eq.(2):

$$p_{i,t}^{heat} = \frac{p_{i,t}^{H_2}}{U_{tn}(T_{i,t})}(U_{cell}(\frac{p_{i,t}^{H_2}}{U_{tn}(T_{i,t})}, T_{i,t}) - U_{tn}(T_{i,t})) \tag{2}$$

$T_{i,t}$ is working temperature of the electrolyser, U_{cell} is operating cell voltage and U_{tn} is thermoneutral voltage[3]. eq.(2) illustrates that the temperature $T_{i,t}$ determines the output proportion of $p_{i,t}^{\mathrm{H_2}}$, $p_{i,t}^{\mathrm{heat}}$ produced by the electricity from the electricity network. However, because $p_{i,t}^{\mathrm{H_2}}$, $p_{i,t}^{\mathrm{heat}}$ and their proportions are state variables, it is impossible to integrate them into a convex linear optimization model by multiplying the two variables. Therefore, using parameters from [12], [3] demonstrate their relationship by showing the feasible operational area of an alkaline electrolyser, which is a slightly curved surface. Along the two diagonals of the rectangular curved surface operational area, divide the surface into four triangles [3]. To formulate the optimization problem, we use big M method to express it, where M is a large enough constant. In addition,a_j^k is convex combination coefficient,δ_j is the selection coefficient and N represents the corners of the area. Therefore, for $\forall j \in \sigma_{\mathrm{ABCD}}$ (j represents one of the areas in σ_{ABCD} and N_j represents the corners of the area j), we can design the following dispatch model to gain $p_{i,t}^{\mathrm{H_2}}$, $p_{i,t}^{\mathrm{heat}}$ and $T_{i,t}$:

$$\begin{cases} 0 \le \sum_{k=1}^{N_j} a_j^k x_j^k \le \delta_j \mathrm{M} \\ 0 \le \sum_{k=1}^{N_j} a_j^k y_j^k \le \delta_j \mathrm{M} \\ 0 \le \sum_{k=1}^{N_j} a_j^k z_j^k \le \delta_j \mathrm{M} \\ \sum_{k=1}^{N_j} a_j^k = 1, 0 \le a_j^k \le 1 \\ \sum \delta_j = 1, \delta_j \in \{0,1\} \end{cases} \tag{3}$$

$$\begin{cases} p_{i,t}^{\mathrm{H_2}} = \sum^{\forall j \in \sigma_{\mathrm{ABCD}}} \sum_{k=1}^{N_j} a_j^k x_j^k \\ T_{i,t} = \sum^{\forall j \in \sigma_{\mathrm{ABCD}}} \sum_{k=1}^{N_j} a_j^k y_j^k \\ p_{i,t}^{\mathrm{heat}} = \sum^{\forall j \in \sigma_{\mathrm{ABCD}}} \sum_{k=1}^{N_j} a_j^k z_j^k \end{cases} \tag{4}$$

2.1.2 Thermal submodel: The thermal submodel describes a mathematical model of the exchange of the electrolysers and thermal networks. According to [13], thermal dynamics determine the working temperature $T_{i,t}$ by controlling the output heat $q_{i,t}, i \in EL$:

$$\Delta T_{i,t} = \frac{\Delta t}{\mathrm{C_t}}\left(p_{i,t}^{\mathrm{heat}} - p_{i,t}^{\mathrm{loss}} - \frac{q_{i,t}}{\eta_{i,2}}\right) \tag{5}$$

$$p_{i,t}^{\mathrm{loss}} = \frac{1}{\mathrm{R_t}}(T_{i,t} - \mathrm{T_a}) \tag{6}$$

$\eta_{i,2}$ is the efficiency of the heat exchanger and $p_{i,t}^{\mathrm{loss}}$ is power loss to air at time t. Specific values of $\mathrm{C_t}$ and $\mathrm{R_t}$ are introduced in [3].

The $\underline{T_i}$ and $\overline{T_i}$ is the lower and upper limits of the working temperature, respectively. The working temperature is a state variable that should meet its constraint:

$$\underline{T_i} \le T_{i,t} \le \overline{T_i} \tag{7}$$

As the water electrolysis process changes the working temperature $T_{i,t}$, which can be seen as a way to store heat, the whole electrolyser is a device for heat storage.

2.2 Hydrogen storage tank

According to [14], the hydrogen molar flow produced by the electrolyser can be expressed as a function of $p_{i,t}^{\mathrm{H}_2}$:

$$n_{i,t} = \frac{p_{i,t}^{\mathrm{H}_2} \Delta t}{\mathrm{LHV}_{\mathrm{H}_2}}, i \in EL \tag{8}$$

Regarding the hydrogen tank, an important control variable is the hydrogen tank pressure, which can be expressed by the ideal gas law [14]:

$$\Delta Pr_{i,t} = \frac{RT_i}{V_i} n_{i,t}, i \in HS \tag{9}$$

and the pressure has the following limits:

$$\underline{Pr_i} \leq Pr_{i,t} \leq \overline{Pr_i} \tag{10}$$

It is noteworthy that the ideal gas law can be used by setting a relatively low maximum hydrogen pressure (13.8 bar) and the average temperature inside the hydrogen tank T_i is assumed to be constant (313 K).

2.3 Oxygen-enriched gas purification

The UK requires that the purity of medical oxygen must exceed 99.5%, and the impurities should be harmless to the human body. Currently, cryogenic separation is the mainstream method of manufacturing medical oxygen [15]. Utilizing the different boiling points of the different gases, cryogenic separation distills off oxygen from the air by lowering the temperature. This method can produce medical oxygen stably, but it is expensive [7].

The oxygen-enriched gas generated from the electrolyser can produce medical oxygen through purification process. The oxygen-enriched gas has only two impurities, H_2 and H_2O, and the catalyst can synthesize H_2 and O_2 into H_2O. Therefore, as long as using the molecular sieve to filter H_2O, high-purity medical oxygen is obtained. A comparison of cryogenic separation and oxygen-enriched gas purification is provided in Fig. 2. From the data perspective, the comparison of the efficiency of the two methods is provided in Table 1.

Table 1 Efficiency comparison

	Oxygen-enriched gas purification	Cryogenic separation
Oxygen purity	99.999%[17]	99.5%−99.9%
Energy cost(wh/g)	0.04	0.61[7]
impurities	H_2 and H_2O	N_2,Ar,CO_2, and etc.

Table 1 shows that oxygen-enriched gas purification can produce higher purity of oxygen, which meets the UK medical oxygen standards, at a lower cost. The reason for this is that the oxygen purity of the oxygen-enriched gas reaches 98.5% and the impurity types are relatively few. In comparison, air oxygen purity is only 21%, and it contains many different types of impurities. The reason that oxygen-enriched gas purification is not currently used is that electrolysing water requires a large amount of electricity. However, in an IES, hydrogen has been produced by electrolysing water and, when hydrogen is produced, the by-product, oxygen-enriched gas, is produced at the same time. Therefore, the price of oxygen-enriched gas purification is relatively low.

In addition, the cost of purchasing devices for cryogenic separation is much higher than that required for oxygen-enriched gas purification, which requires only one oxygen-enriched gas purification unit. Comparatively, the cryogenic separation method requires many different items of device,

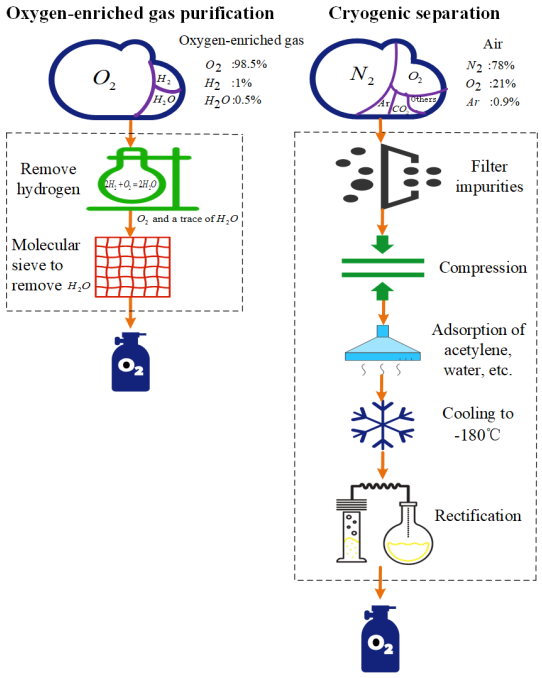

Fig. 2: Comparation of cryogenic separation and oxygen-enriched gas purification

including compressors, filters and distillation towers, which impose additional labour costs. Besides, it is worth mentioning that distillation towers are usually tall and, hence, cryogenic separation requires more floor-space than oxygen-enriched gas purification.

Because oxygen-enriched gas purification is cheap in both operational costs and device costs, it is a better choice than cryogenic separation to produce medical oxygen.

The model of oxygen-enriched gas purification is as shown in eq.(11). The cost of oxygen-enriched gas purification C_{PO} is the total weight of oxygen produced per day PO multiplied by the cost of purification r_{O2}.

$$C_{PO} = PO \cdot r_{O2} \tag{11}$$

3 IPHHOO model formulation

To improve IES economic by P2HO system, we propose the IPHHOO model. IPHHOO formulates the operation of power, heating, hydrogen and oxygen systems as a mixed integer optimization problem, taking into consideration various constraints in system operation, including load balance, reserve requirements, ramping limits, and etc. It optimizes the hourly power, heat, hydrogen and oxygen output of all controllable generation resources with the objective of minimizing the operational costs for the energy supplier.

Although this paper focuses on the economic impact of the combined production of hydrogen and oxygen on IES operation, for completeness and generality, the IES in this section includes commonly used devices such as electric boilers, combined heat and power (CHP), thermal power plants, electrolysers, hydrogen storage tanks, power storage devices, renewable power units, etc. The structure of this section is shown below. First, this section introduces the overall structure of the system in section 3.1. Second, the objective function and constraints will be given in section 3.2 and 3.3.

Thirdly, the description and model of other devices will be given in section 3.3-3.6 separately.

3.1 System structure

System structure and the energy flow are shown in Fig. 3. Thermal power plants, CHP units, and renewable power generate electricity. Electric boilers and CHP generate heat and, in addition, the electrolyser can be regarded as a heat storage tank [3]. Electrolyser produces hydrogen to supply fuel cell vehicles and natural gas pipelines through hydrogen storage tanks. The oxygen-enriched gas from the electrolyser is purified, bottled, and transported to the hospital.

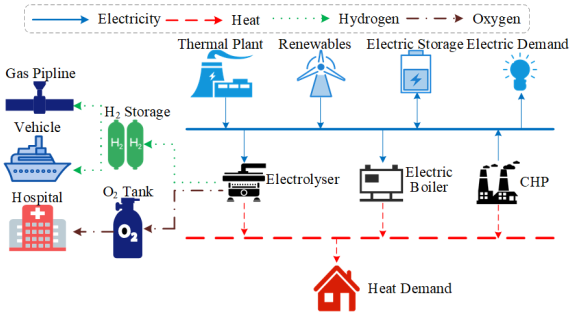

Fig. 3: System structure of the IES considering oxygen-enriched gas purification

3.2 Objective function

The objective aims to minimizing the operational costs for the energy supplier. We assume that when the hydrogen and medical oxygen produced by electrolyser are insufficient to meet demand, they must be purchased externally at a higher price. The objective is shown as follow:

$$\min C_{fuel} + C_{curtail} + C_{BH} + C_{BO} + C_{PO} - P_{SO} - P_{SH} \tag{12}$$

where C_{fuel} is the total fuel cost and C_{curtail} is a penalty term for the curtailed amount of renewable power. C_{BH} and C_{BO} are the costs of purchasing H_2 and O_2, respectively.

P_{SH} and P_{SO} are the profits from selling excess H_2 and O_2, respectively.

Here, we consider C_{fuel} as the total fuel cost of all thermal power plants (C_{TP}) and CHP units (C_{CHP}) [4]. The cost of thermal power plants and of CHP units are formulated in eq.(13) and (14), respectively. The cost of a conventional thermal power plant unit is modelled as linear to its energy output $p_{i,t}^{TP}$ and the price rate of unit i is r_i. The cost of a CHP unit was discussed in the subsection 3.3.5.

$$C_{TP} = \sum_{t=1}^{T_h} \sum_{i \in TP} p_{i,t}^{TP} \cdot r_i \tag{13}$$

$$C_{CHP} = \sum_{t=1}^{T_h} \sum_{i \in CHP} c_{i,t} \tag{14}$$

The penalty term C_{curtail}, as shown in eq.(15), is the sum of the difference between the actual renewable power integrated in the power system $p_{i,t}^{R}$ and expected maximum outputs from all renewable power generation $\widehat{P_{i,t}}$, multiplied by renewable power penalty factor β.

$$C_{\text{curtail}} = \beta \sum_{t=1}^{T_h} \sum_{i \in W} (\widehat{P_{i,t}} - p_{i,t}^{R}) \tag{15}$$

The costs of additional hydrogen and oxygen purchases, C_{BH} and C_{BO}, respectively are the weight of the purchase BH_t,BO multiplied by the price r_H,r_{O1}, as shown in eq.(16) and (17), respectively.

$$C_{BH} = \sum (BH_t \cdot r_H) \tag{16}$$

$$C_{BO} = BO \cdot r_{O1} \tag{17}$$

Similarly, the profit from selling hydrogen and oxygen is shown below:

$$P_{SH} = \sum (n_t^{EL} + BH_t - DH_t) \cdot r_H \tag{18}$$

$$P_{SO} = (PO + BO - DO) \cdot r_{O1} \tag{19}$$

DH_t is the hydrogen demand at time t and DO is the total medical oxygen demand.

3.3 Constraints

This system constraints include the real-time balance for power, heat, hydrogen, reserve requirements and other restrictions of the various devices employed in the system.

3.3.1 Power and heat balances: The electric power balance is formulated in eq.(20). The system demand DP_t equals the summation of electric power generated from all units, minus the power consumed by electric boilers and the charging power required for electrical energy storage and electrolysers. Note that $p_{i,t}$ is negative when unit i consumes power.

$$\sum_{i \in \{TP,CHP,W,EB,ES,EL\}} p_{i,t} = DP_t, \forall t \tag{20}$$

The heat balance is formulated in eq.(21). The heat demand DQ_t equals the summation of heat generated from CHP units, electric boilers and electrolyser.

$$\sum_{i \in \{CHP,EB,EL\}} q_{i,t} = DQ_t, \forall t \tag{21}$$

3.3.2 Hydrogen and oxygen balances: The hydrogen balance is formulated in eq.(22). The amount of hydrogen produced n_t^{EL} plus the amount of hydrogen purchased BH_t minus the amount of hydrogen sold SH is equal to the hydrogen demand storage tanks and purchases:

$$DH_t = n_t^{EL} + BH_t - SH \tag{22}$$

The oxygen constraint is formulated in eq.(23). The oxygen demand equals the sum of the oxygen generated from electrolysers plus any oxygen purchased minus the amount of oxygen sold SO:

$$DO = 0.5 \times n^{EL} + BO - SO \tag{23}$$

3.3.3 System reserve constraint: The system reserve ensures that the schedules of units can provided sufficient electric power in real time. According to [4], this constraint is formulated as:

$$\sum_{i \in TP \cup CHP} \overline{P_i} \cdot u_{i,t} + \xi \sum_{i \in W} \widehat{P}_i \geq DP_t(1+\epsilon), \forall t \tag{24}$$

Parameters ξ and ϵ are set by the system operator based on the historical performance of the renewable units and system requirements, respectively.

3.3.4 Flexibility constraints: There are ramping constraints for conventional thermal power plants and CHP units. Based on [4], for $\forall t, i \in TP \cup CHP$, these constraints are as follows:

$$p_{i,t} - p_{i,t-1} \leq RU_i \cdot u_{i,t-1} + SU_i \cdot (u_{i,t} - u_{i,t-1}) \quad (25)$$

$$p_{i,t} - p_{i,t-1} \geq -RU_i \cdot u_{i,t-1} - SD_i \cdot (u_{i,t} - u_{i,t-1}) \quad (26)$$

$$\underline{P_i} \cdot u_{i,t} \leq p_{i,t} \leq \overline{P_i} \cdot u_{i,t} \quad (27)$$

Based on [4], the constraints of minimum ON and OFF time are formulated as follows:

$$\sum_{t=1}^{G1_i} (1 - u_{i,t}) = 0 \quad (28)$$

$$\sum_{t=j}^{j+UT_i-1} u_{i,t} \geq UT_i \cdot (u_{i,j} - u_{i,j-1}), \quad \forall j \in [G1_i + 1, T_h - UT_i + 1] \quad (29)$$

$$\sum_{t=j}^{T_h} \big(u_{i,t} - (u_{i,j} - u_{i,j-1})\big) \geq 0, \quad \forall j \in [T_h - UT_i + 2, T_h] \quad (30)$$

Equations (28)–(30) describe the ON time limit, where UT_i is the minimum ON time of unit i and $G1_i$, which is associated with the initial status of unit i, represents the consecutive ON time intervals required before it can be shut down:

$$\sum_{t=1}^{G0_i} u_{i,t} = 0 \quad (31)$$

$$\sum_{t=j}^{j+DT_i-1} (1 - u_{i,t}) \geq DT_i \cdot (u_{i,j-1} - u_{i,j}), \quad \forall j \in [G0_i + 1, T_h - DT_i + 1] \quad (32)$$

$$\sum_{t=j}^{T_h} \big(1 - u_{i,t} - (u_{i,j-1} - u_{i,j})\big) \geq 0, \quad \forall j \in [T_h - DT_i + 2, T_h] \quad (33)$$

Meanwhile, eq.(31)–(33) describe the OFF time limit, where DT_i is the minimum OFF time of unit i and $G0_i$, which is associated with the initial status of unit i, represents the consecutive OFF time intervals required before it can be start up.

3.3.5 CHP modelling: The heat and electric power production are coupled for CHP units. The concept of a feasible operational region has been widely adopted to describe the operational characteristics of a CHP unit. The boundaries of the region reflect the internal operational limitations of a CHP unit, such as the steam pressure limits of turbines and the fuel limits of boilers. The number of boundaries of CHP unit i is denoted by K_i and the heat output, electricity output, cost of CHP unit i and the combination coefficients is denoted by $q_{i,t}, p_{i,t}, c_{i,t}, \alpha_{i,t}^k$ respectively.

Here, we apply a linearized model that formulates the fuel cost, electric power, and heat outputs of the CHP units with the following convex feasible operational area [11]:

$$\begin{cases} q_{i,t} = \sum_{k=1}^{K_i} \alpha_{i,t}^k x_i^k \\ p_{i,t} = \sum_{k=1}^{K_i} \alpha_{i,t}^k y_i^k \\ c_{i,t} = \sum_{k=1}^{K_i} \alpha_{i,t}^k z_i^k \\ \sum_{k=1}^{K_i} \alpha_{i,t}^k = 1, 0 \leq \alpha_{i,t}^k \leq 1 \end{cases}, i \in CHP \quad (34)$$

3.3.6 Electric boiler modelling: In this paper, heat generated from electric boiler i holds a linear relationship with the electric power consumed by this boiler. The conversion efficiency is denoted by $\eta_i, i \in EB$:

$$q_{i,t} + \eta_i p_{i,t} = 0, i \in EB, \forall t \quad (35)$$

$$0 \leq -p_{i,t} \leq \overline{P_i}, i \in EB, \forall t \quad (36)$$

3.3.7 Electricity storage device modelling: A simplified electrical storage model is shown in eq.(37) and (38). The model considers the same inlet/outlet efficiencies as in $\eta_i, i \in ES$ and the same maximum charging/discharging rates as in $\overline{P_i}$ and $\underline{P_i}, i \in ES$. In addition, $\Delta p_{i,t}$ is the change of electrical energy in electrical storage device and $p_{i,t}$ is the electrical output of electrical storage device. When $u_{i,t}$ is 1, the electrical storage device is charged, and when $u_{i,t}$ is 0, the electrical storage device is discharged. It incorporates the constraints imposed by limitations on the maximum and minimum volumes, as $\overline{ES_i}$ and $\underline{ES_i}, i \in ES$, respectively [16].

$$\begin{cases} (1 - u_{i,t})\underline{P_i} \leq \Delta p_{i,t} \leq u_{i,t}\overline{P_i} \\ -u_{i,t}\mathrm{M} \leq p_{i,t} + \eta_i^{\mathrm{dc}} \Delta p_{i,t} \leq u_{i,t}\mathrm{M} \\ (u_{i,t} - 1)\mathrm{M} \leq p_{i,t} + \Delta p_{i,t}/\eta_i^{\mathrm{ch}} \leq (1 - u_{i,t})\mathrm{M} \end{cases} i \in ES, \forall t \quad (37)$$

$$\underline{ES_i} \leq \sum_{t=1}^{j} \Delta p_{i,t} \leq \overline{ES_i}, i \in ES, \forall j \in [1, T_h] \quad (38)$$

4 Case study

4.1 Test system

In this section, we design a test system based on the actual situation in TaiZhou to evaluate the effectiveness of the IPH-HOO model. In TaiZhou, located in Jiangsu Province, China, there is a China Medical City and strong potential demand for hydrogen and medical oxygen.

As shown in Fig. 4, the China Medical City, a national pharmaceutical high-tech park, divides TaiZhou into two residential areas, Hailing district (district I) and Gaogang district (district II). The IES of the Medical City needs to supply power and heat to both districts at the same time. In addition, hydrogen will be supplied to the port to meet the demand for hydrogen fuel cell ship and the purified oxygen will be bottled in the Medical City. The test system is shown as follows.

As shown in Fig. 5, there are two same CHP units that serve two independent heating districts. District I is served by CHP1, together with a P2H system and a 20-MW electric boiler, with a 20-MW electrical energy storage coupled to this system. District II is served by CHP2, along with a 25-MW electric boiler.

The hourly demands for electric power, heat and hydrogen in the test system are shown in Fig. 6. The electric demand,

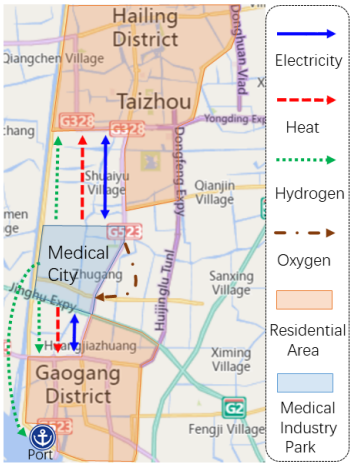

Fig. 4: TaiZhou integrated energy supply map

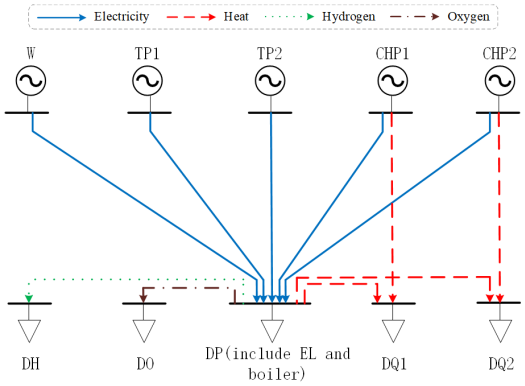

Fig. 5: Test system of integrated power, heat, hydrogen and oxygen optimization model

hydrogen demand and wind generation have similar daily trends to [11, 20]. This case study does not take the uncertainty of wind resource into account. The hydrogen demand has three sources: demand for hydrogen fuel cell cars, demand for hydrogen fuel cell ships and demand for natural gas doped with hydrogen. The demand data for hydrogen fuel cell cars are derived from[21] and the demand for hydrogen fuel cell ships is considered to be similar to that for hydrogen fuel cell cars. The maximum hydrogen demand for both types is 120 kg/h and the demand is concentrated at commuting times. The demand data for natural gas doped with hydrogen was calculated based on a 2% doping ratio. According to a reasonable estimate of the amount of natural gas used in TaiZhou Medical City, the peak value of hydrogen used for doping is 100 kg/h. Additionally, the demand data for medical oxygen is 480kg/day, which is calculated based on an average of 1,400 bottles of oxygen consumed per 500 beds per month[22].

The market price of hydrogen obtained from [18] and the price of medical oxygen is obtained from PharmaCompass[19]. The price of hydrogen is 112 yuan/kg and the price of medical oxygen is 70 yuan/kg. The electricity cost for purifying oxygen is calculated from the power used by the QNCB series oxygen-enriched gas purification unit of the China Shipbuilding Industry Corporation' s 718th Research Institute and the TaiZhou electricity price[17]. The cost of purifying the oxygen-enriched gas is only 0.016 yuan/kg. The reason

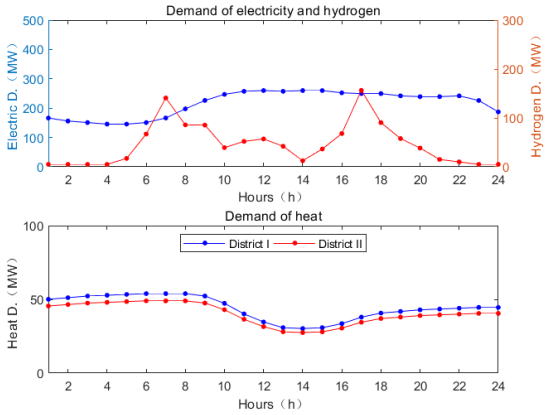

Fig. 6: Demand for electric power, heat and hydrogen

why the cost of purified oxygen is so low was illustrated in detail in Section 2.7. The wind curtailment coefficient is 100yuan/MWh.

Table 2 Generating unit data

	TP		CHP	
	1	2	1	2
Max output(MW)	110	50	80	80
Min output(MW)	10	5	30	30
Ramping up limit(MW/h)	4	5	5	5
Ramping down limit(MW/h)	4	5	5	5
Start up limit(MW/h)	5	8	8	8
Shut down limit(MW/h)	5	8	8	8
min up time(h)	3	2	2	2
min down time(h)	3	2	2	2
initial status(MW)	10	5	45.6	45.4

Based on the above data, this paper uses *Yalmip* calling *Gurobi* to seek the most economic unit dispatch strategy.

4.2 Simulation results

To demonstrate the economic value of the proposed method, we designed and simulated three cases. An expenditure comparison of these three cases is shown in Table 3.

Table 3 Expenditure comparison

Number	Cases	Expenditure
1	Both O_2 and H_2 depend on purchase	1638331
2	EL to produce H_2,purchase O_2	1284614
3	EL to produce H_2,purification to produce O_2	278932

In case 1, TaiZhou City needs to purchase 2202.4 kg of H_2 and 4,123.2 kg of medical O_2 to meet its own demand, which costs 246,668.8 yuan and 288,624 yuan, respectively.

In case 2, TaiZhou only needs to purchase medical O_2, which costs 288,624 yuan. In addition to meeting their own H_2 needs, the P2H system allows TaiZhou to sell its excess H_2, which yields a profit of 156,536 yuan. However, working with a full load, the electrolyser uses an extra 180 MWh of electricity, which costs 80,100 yuan.

In case 3, the electrolyser produced a total of 14,400 kg of medical O_2. After retaining 4,123.2 kg for its own needs, TaiZhou has 10,277.8 kg of O_2 that can be sold, which yields

a profit of 719,376 yuan. Furthermore, the total cost of producing 144,00 kg of medical O_2 with oxygen-enriched gas is only 72 yuan. The sales of medical O_2 can earn a significant profit because O_2 is usually sold by weight. Although the electrolysis of a water molecule can only produce one H_2 and half a O_2, the weight of a O_2 molecule is eight times that of a H_2 molecule. Therefore, the weight of O_2 produced by P2H is four times that of H_2 while medical O_2 is not cheap. Hence, the combined production of H_2 and medical O_2 improves the economics of IES significantly.

The electric output of each unit in the three cases is shown below.

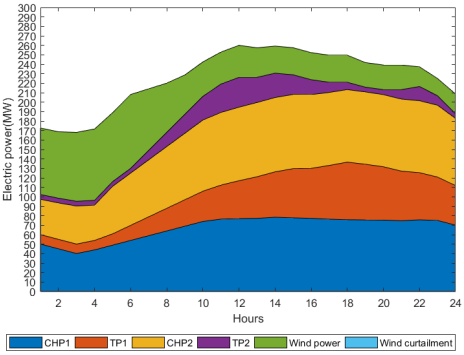

Fig. 7: Electric output of each device of case 1

When both O_2 and H_2 depend on external purchases, there is no need to produce O_2 and H_2 and, hence, the electrolyser works under a light load and serves only as a heat source and heat storage tank. As shown in Fig. 7, the electrolyser works only at 6 am for heating and the output of the power supply unit has a spike at 6 am. Naturally, the electrolyser consumes less power and thus, the output of CHP and TP is less than in the other cases. On account of the low output of TP and CHP, the fuel cost is relatively lower than in the other cases. However, buying O_2 and H_2 is expensive, so the expenditure is more than of other cases. In addition, because the test system is flexible, and the electrolyser can absorb excess wind power, case 1 does not have wind curtailment.

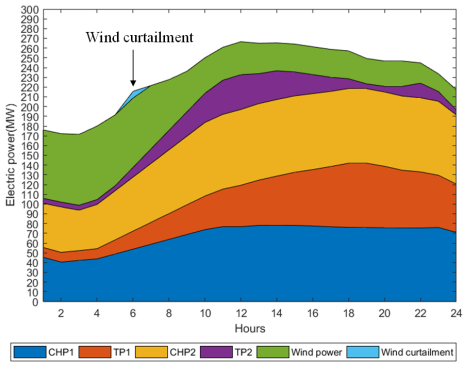

Fig. 8: The electric output of each device of case 2

As shown in Fig. 8, when using the electrolyser to produce H_2 and purchasing O_2, the electrolyser works with a full load, which consumes an extra 7.5 MW. However, the power consumed by the boiler decreases because the electrolyser can be seen as a device for heat source and heat storage. In general, the outputs of TP and CHP increase slightly. Despite the fuel cost increases, there is no need to purchase H_2, which more than offsets the rise in fuel costs. Hence, the expenditure in case 2 is even less than in case 1. In addition, due to ramping constraints for conventional thermal power plants and CHP units, and the electrolyser has been working for 24 hours, no additional electrical load can be found at 6 am to absorb excess wind power. Hence, at 6 am, there is a little wind curtailment.

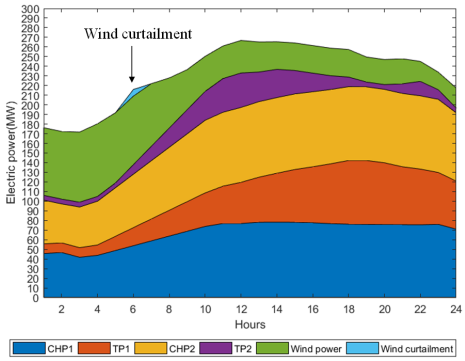

Fig. 9: Electric output of each device of case 3

As shown in Fig. 9, when using purification to produce O_2, the electrolyser works with a full load and produces 14,400 kg of medical O_2. At the same time, the purification of O_2 requires an additional 0.288 MW of electricity. Hence, the output of CHP and TP has increased by 0.288 MW. Selling excess O_2 can result in large profits, making the expenditure in case 3 surprisingly low.

Obviously, the method proposed in this paper is both effective and economical.

4.3 Sensitivity analysis

In reality, the demand for H_2 fluctuates with the external environment. Hence, we analysed the sensitivity of the expenditure to the demand for H_2.

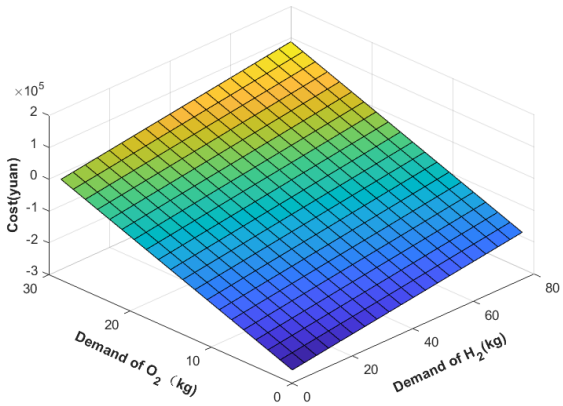

Fig. 10: Sensitivity analysis of demand for H_2 and O_2

Fig. 10 shows the changes in expenditure when H_2 demand changes. Expenditure is equal to cost minus profits. Because the profit from selling medical O_2 and H_2 is highly attractive

and the cost of producing medical O_2 and H_2 with excess wind power is very cheap, the electrolyser has been working under a full load to produce more medical O_2 and H_2. However, the more demand there is for H_2 and O_2, the less H_2 and O_2 can be sold. Hence, expenditure decreases in an approximately linear manner as demand for H_2 and O_2 increases.

After adding oxygen purification into IES, the profit may be greater than the cost, which means the expenditure is negative. In addition, the price of H_2 and O_2 fluctuates with the market. Therefore, Fig. 11 shows the sensitivity of the expenditure to the price of H_2 and O_2:

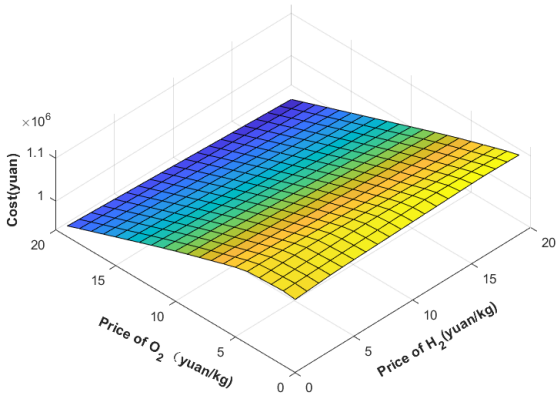

Fig. 11: Sensitivity analysis of price of H_2 and O_2

When the price of H_2 and O_2 is zero, all the demand for H_2 and O_2 is met by purchase. Hence, in the beginning, when the price of H_2 and O_2 rises, so does the expenditure. However, electrolysing water to produce H_2 and O_2 soon replaces purchase. Therefore, when the prices of H_2 and O_2 rise, so does the profit from selling H_2 and O_2. Thus, expenditure decrease. In addition, as shown in Fig. 11, because the weight of oxygen produced is 4 times that of hydrogen, expenditure is more sensitive to the price of oxygen.

Third, given the great importance that the Chinese government attaches to wind power, we analyse the sensitivity of various costs to maximum output of wind power. The results are presented below.

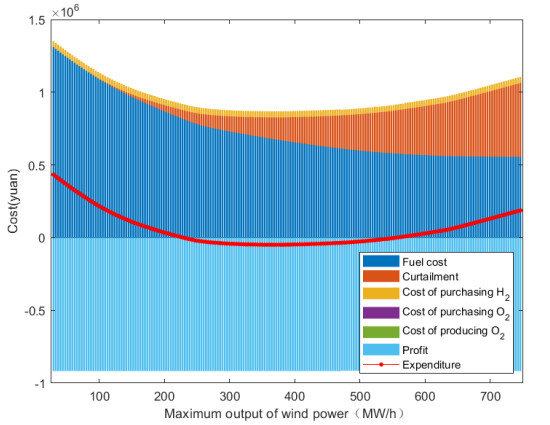

Fig. 12: Sensitivity analysis of wind power

As shown in Fig 12, when the maximum output of wind power increases, the system is not sufficiently flexible to absorb the entire wind power and, therefore, wind curtailment increases significantly. Meanwhile, it is worth noting that with the increase in maximum output of wind power, the reduction in fuel costs becomes slower and slower. Hence, as wind power output increases, the expenditure first decreases but then begins to increase.

Besides, the purification process to produce O_2 can reduce the wind curtailment caused by the increase of wind power. The reason is that as long as the electrolyser is working, it can consume wind power to purify O_2. Last but not least, when the wind curtailment coefficient is high, the electrolyser and oxygen purification system can run at light load before the peak of wind power, and run at full load at the peak of wind power output, which reduces wind curtailment.

5 Conclusion

As oxygen-enriched gas, the by-product of P2H process (electrolysation), has not been utilized before, this paper studied the economic operation of IES which considers the combined production of hydrogen and medical oxygen.

First, we compared oxygen-enriched gas purification and conventional method of producing medical oxygen, the cryogenic separation. We found that oxygen-enriched gas purification can produce higher purity oxygen at a lower price.

Second, we explored a new P2HO system that can utilise oxygen-enriched gas.

Thirdly,we proposed the IPHHOO model to simulate the economic operation of IES considering the combined production of hydrogen and medical oxygen.

Then, we used the IES of TaiZhou City for case study and used *Yalmip* calling *Gurobi* to seek the most economic unit dispatch strategy. The simulation results showed that the combined production of hydrogen and medical oxygen may reduce the operation expenditure of IES.

IPHHOO model may help improve the economics for the IES of areas like TaiZhou in the long run. In addition, at this very moment of the outbreak of COVID-19, IPHHOO model may also help relieve the shortage of medical oxygen demand.

In future, without loss of generality, we plan to explore the application of meta-heuristics optimizer in solving larger scale economic dispatch problem and take the uncertainty of wind resource taken into consideration.

6 Acknowledgements

This research is supported by Nation Science Foundation of China (51907026), Nation Science Foundation of Jiangsu (SBK2019043173), Jiangsu Provincial Key Laboratory of Smart Grid Technology and Equipment, State Key Laboratory of Smart Grid Protection and Control, and State Grid Jiangsu Economic Research Institute.

7 References

1 Pinson, P., Mitridati, L., Ordoudis, C., *et al.*: 'Towards fully renewable energy systems: Experience and trends in Denmark', *CSEE Journal of Power and Energy Systems*, 2017, **3**, (1), pp. 26–35

2 Mitridati, L., Taylor, J.A.: 'Power Systems Flexibility from District Heating Networks'. 2018 Power Systems Computation Conference (PSCC), Dublin, 2018, pp. 1-7.

3 Ge, P., Hu, Q., Wu, Q., *et al.*: 'Increasing Operational Flexibility of Integrated Energy Systems by Introducing Power to Hydrogen', *IET Renewable Power Generation*, 2019, **14**, (3), pp. 372-380

4 Chen, X., McElroy, M.B., Kang, C.: 'Integrated energy systems for higher wind penetration in china: Formulation, implementation, and impacts', *IEEE Transactions on Power Systems*, 2018, **33**, (2), pp. 1309–1319

G. Petrecca and M. Decarli, "A review of hydrogen applications: Technical and economic aspects," MELECON 2008 - The 14th

IEEE Mediterranean Electrotechnical Conference, Ajaccio, 2008, pp. 658-662.
5 Petrecca, G., Decarli,M., 'A review of hydrogen applications: Technical and economic aspects', *IEEE Mediterranean Electrotechnical Conference*, Ajaccio, 2008, pp. 658-662.
6 Mendis, N.,Muttaqi,K., Perera, S., *et al.*: 'An Effective Power Management Strategy for a Wind–Diesel–Hydrogen-Based Remote Area Power Supply System to Meet Fluctuating Demands Under Generation Uncertainty', *IEEE Transactions on Industry Applications*, 2015, **51**,(2), pp. 1228-1238
7 Li, J.: 'Optimization and retrofitting of air separate unit: case study of company A', *MS diss.*, South China University of Technology
8 'Number of Infected Persons', https://www.chinadaily.com.cn/a/202006/18/WS5eea97a1a310834817253c1f.html,accessed 19 June 2020
9 'Patients need Oxygen', https://global.chinadaily.com.cn/a/202006/17/WS5ee8fb3ca3108348172537a1.html,accessed 19 June 2020
10 'Patients need Oxygen', https://thefrontierpost.com/kabul-hospitals-lack-oxygen-to-treat-covid-19/,accessed 19 June 2020
11 Chen, X., Kang, C., O'Malley, M., *et al.*: 'Increasing the flexibility of combined heat and power for wind power integration in china: Modeling and implications', *IEEE Transactions on Power Systems*, 2015, **30**, (4), pp. 1848–1857
12 Koponen, J.: 'Review of water electrolysis technologies and design of renewable hydrogen production systems'. Msc thesis, Lappeenranta University of Technology, 2015
13 Valverde, L., Rosa, F., Del Real, A. J., *et al.*: 'Modeling, simulation and experimental set-up of a renewable hydrogen-based domestic microgrid', *International Journal of Hydrogen Energy*, 2013, **38**, (27), pp. 11672–11684
14 Cau, G., Cocco, D., Petrollese, M., *et al.*: 'Energy management strategy based on short-term generation scheduling for a renewable microgrid using a hydrogen storage system', *Energy Conversion and Management*, 2014, **87**, (107), pp. 820–831
15 'cryogenic separation', https://www.51g3.com.cn/lyhsyqtgs/newslist_161843.html,accessed 20 January 2020
16 Zhao, H., Wu, Q., Hu, S., *et al.*: 'Review of energy storage system for wind power integration support', *Applied energy*, 2015, **137**, pp. 545–553
17 ' oxygen-enriched gas purification device', http://www.peric718.com,accessed 16 January 2020
18 'Hydrogen price', https://coinmarketcap.com/currencies/hydrogen/,accessed 20 January 2020
19 'Oxygen price', https://www.pharmacompass.com/price/oxygen,accessed 20 January 2020
20 'Demand Data', http://motor.ece.iit.edu/data/6bus_Data_DR.pdf,accessed 25 April 2019
21 El-Taweel, N.A., Khani, H., Farag, H.E.Z.: 'Hydrogen storage optimal scheduling for fuel supply and capacity–based demand response program under dynamic hydrogen pricing', *IEEE Transactions on Smart Grid*, 2018, pp. 1–12
22 'Oxygen Demand', https://wenku.baidu.com/view/b32440d1cd22bcd126fff705cc17552706225e7d.html,accessed 20 January 2020